Seismic characterization of the Woodford shale in the Anadarko basin

Nabanita Gupta, Supratik Sarkar, and Kurt J. Marfurt, University of Oklahoma*

Summary

Seismic analysis plays a very important role in the characterization of shale gas reservoirs. Several seismic attributes including curvature and coherence attributes are commonly used to highlight discontinuities (Marfurt, 2010). But very often, the complexity of the discontinuity pattern is not clearly seen in these attributes. At the same time, studying the discontinuity patterns along with stratigraphic changes can also provide important clues for shale gas exploration. For the current study, we analyzed the Woodford Shale in the Anadarko basin (Figure 1) with the aid of some newly developed geometric attributes including reflector convergence and reflector rotation along with some common attributes including coherence, curvature and coherent energy.

Introduction

Characterization of gas-shale reservoirs is challenged by its highly heterogeneous nature along with the lack of knowledge about these rocks. Seismic attributes help to illuminate field-scale geomorphologic features as well as building the basin-wide stratigraphic interpretations. Our goal is to identify potential sweet spots in new acreage and bypassed pays in old acreage through careful analyses of seismic attributes in combination with well logs and production data.

Figure 1: Geologic provinces of Oklahoma (Johnson, 2008). Study area covers the Woodford Shale in the Anadarko Basin. Asterisk represents the survey location.

Stratigraphic analyses

The late Devonian-early Mississippian Woodford Shale was deposited in an epeiric sea covering a wide area in the southern midcontinent. The lower boundary of the Woodford is demarcated by a wide spread unconformity developed on top of the Ordovician Hunton Limestone. Co-rendering the coherent energy attribute with inline energy gradient attribute reveals depositional pattern and textures. Such analysis along stratal slices within the Woodford interval showed a broad transgressive event above the Hunton unconformity (Figure 2) showing monotonous low energy pattern throughout the basin (Figure 2b). A couple of patches with subtle energy increase are seen within the monotonous pattern specially near the top of Woodford (Figure 2c) are interpreted as high concentration of siliceous material resulting from the deposition of biogenic chert, as reported in the literature (Lambert, 1993). As the

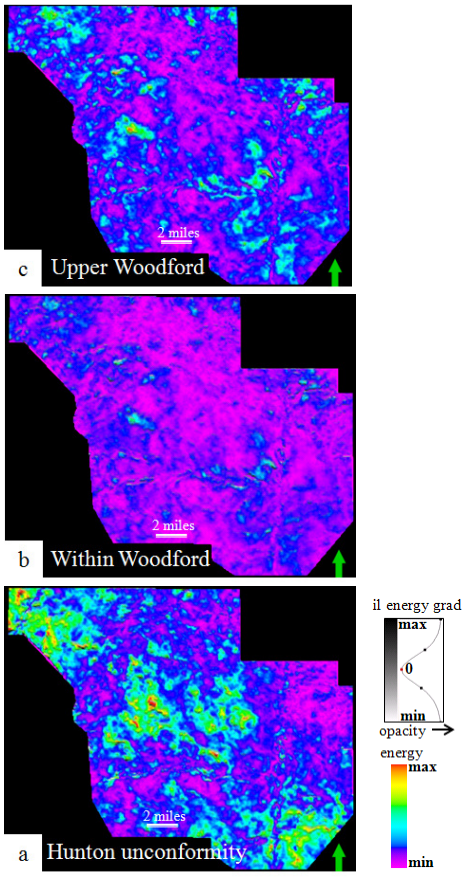

Figure 2: Stratal slices generated by co-rendering coherent energy with in-line energy gradient. Figures from bottom to top represent top of the Hunton unconformity, in the middle of the Woodford Formation and near the top of the Woodford Formation respectively (a, b, c). Notice the subtle high energy nature of the (represented by cyan color) in the top most stratal slice (c) may be indicative of richness in biogenic silica concentration as reported in the literature.

transgressive event continues, these patches are interpreted as increase in biogenic chert deposition, which increases the fracturability of the strata.

Another important feature within the Woodford interval is the effect of some karst features generated within the Hunton interval. We delineate some karst features with the help of geometric attributes along time slices near the top of the Hunton. In Figure 3, we show that co-rendering the most positive curvature with energy ratio similarity help us to delineate the karst features. Plotting shape index modulated by curvedness (Figures 4a and b) blended with the coherence anomaly provides a clearer picture helping us to map the karst features continuing within the Woodford interval.

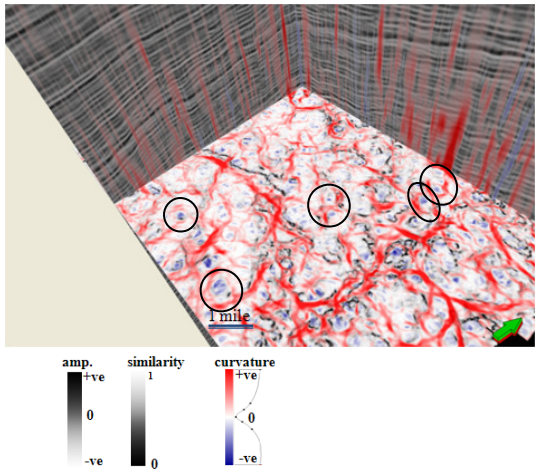

Figure 3: Chair display of a time slice at t =2.298s through most positive principal curvature co-rendered by coherence. The vertical display is a blended image of seismic amplitude and the most positive curvature. The zero curvature values or the planner areas are made transparent. Black circles are representing karst areas in figure.

Marfurt and Rich (2010) introduced a vector reflector convergence attribute to identify stratigraphic patterns including onlap, downlap, and pinchouts. In our dataset, we could map a zone where the strata onlaps progressively onto a possible basin-bounding fault (Figure 5a). The time slice from reflector convergence azimuth modulated by reflector convergence magnitude (Figures 5 a and b) allow us to map the onlap patterns against the possible basin bounding fault and then to build the regional stratigraphic framework.

Understanding structure related elements

Suites of seismic attributes are commonly used in the

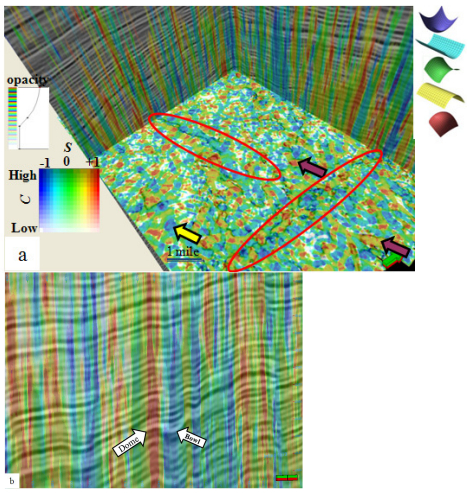

Figure 4a, b: Shape index modulated by curvedness co-rendered with energy ratio similarity. Bowl-shape collapse features possibly associated with the collapse of Hunton Limestone appear blue (yellow arrow). Red (dome) and yellow (ridges) indicate irregularities associated with the unconformity surface (magenta arrow). Note the juxtaposed ridge (yellow and red) and valley (cyan and blue) shaped anomalies on either side of the fault plane marked by red ellipses.

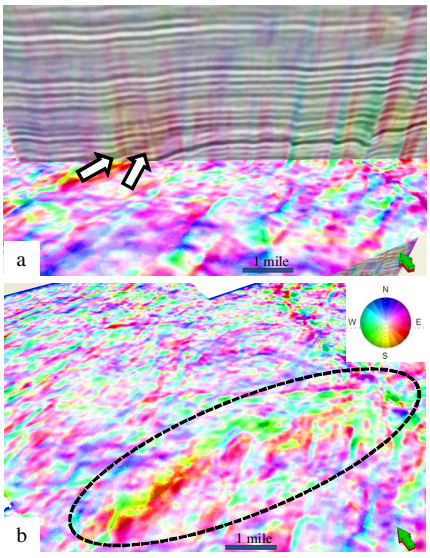

Figure 5: (a) Seismic amplitude on the vertical slice shows the onlap relationship across the possible basin bounding fault (white arrows), whereas vector reflector convergence indicates the direction and magnitude of convergence. Time slice of vector reflector convergence in (a) and (b) indicate changes in onlap direction and magnitude along the fault as indicated by black dotted ellipse in Figure b.

industry to understand and illuminate the discontinuities within the hydrocarbon reservoirs. Attributes including coherence and curvature have been quite useful in the development of the gas-shales. Here we will discuss the utility of some recently developed attributes along with the conventional attributes as we applied those on the Woodford strata.

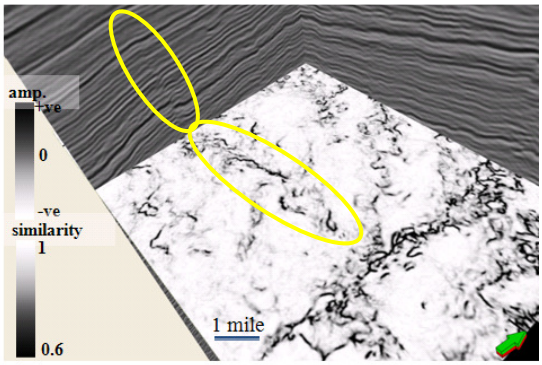

Figure 6: Chair display of a time slice at t = 2.185s through coherence along with vertical display of seismic amplitude. Yellow ellipses show a fault on the vertical seismic and on the time slice.

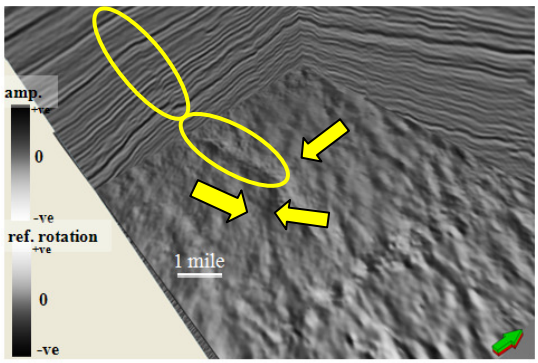

Figure 7: Chair display of a time slice at t = 2.185s through reflector rotation w.r.t. average reflector normal along with vertical slices through seismic amplitude. Yellow ellipses, arrows show a fault along with its branches on the vertical seismic and on the time slice.

Two prominent major fault patterns within our area of interest are closely seen on the coherence time slice (Figure 6). Analyses of time slices generated form reflector rotation about average reflector normal attribute were helpful in delineating those faults which were difficult to pick in the earlier attribute. Figure 7 reveals the displacement with respect to fault as well as the small depression created due to fault related drag in front of the fault. The branching of

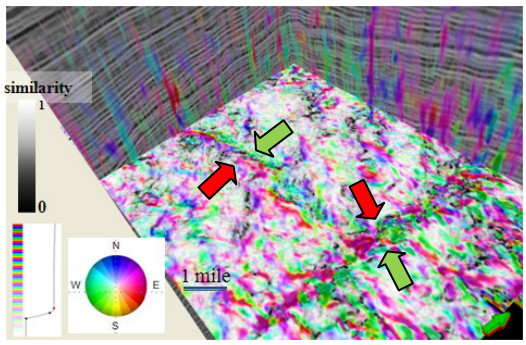

Figure 8: Chair display of a time slice at t = 2.185s through vector reflector convergence, Sobel filter similarity and seismic amplitude. Reflector convergence is displayed against a 2D color wheel. Reflectors that are nearly parallel (low convergence magnitude) are rendered transparent. Note the opposite convergence on either side of rotated fault blocks (marked with red and green arrows).

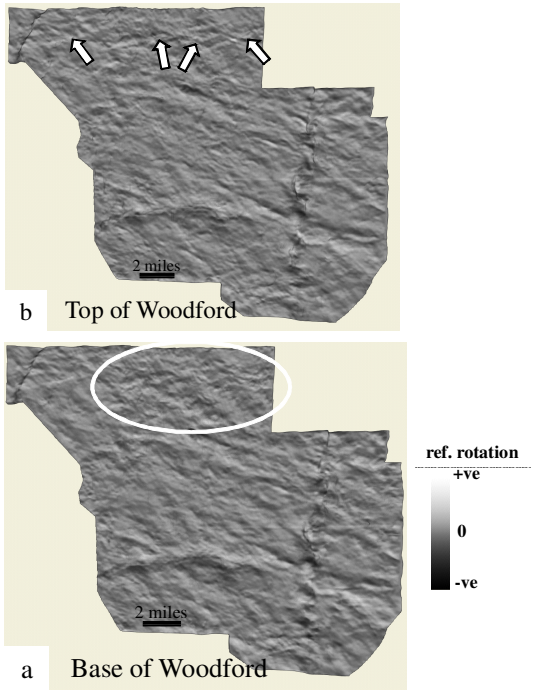

Figure 9: Horizon slices through reflector rotation about the average reflector normal. The horst and graben blocks show considerable contrast and can be interpreted as separate units. (a) Horizon slice at t = 10 ms above the top of Hunton, (b) horizon slice near the top of the Woodford.

the fault is also very clear. Plotting the reflector convergence azimuth modulated by the reflector convergence magnitude, blending with Sobel filter similarity on the same time slice, reveals the rotation of strata and stratal pinch out on either sides of the major E-W fault (Figure 8). It also reveals the patterns within train of faults the N-S direction in the eastern part of the survey.

To understand the fault and lineament orientations and their change in pattern within the Woodford interval, we studied seismic attributes along some horizon slices near the top and bottom of the Woodford interval. Although the pattern remains similar throughout the interval, the orientation show some changes as we move from bottom to top of Woodford interval. In Figure 9a, on a horizon slice 10 ms above the Hunton, reflector rotation about average reflector normal attribute reveals some of those structural patterns. Two major fault system reveals one fault trending N-S and other trending E-W are prominent throughout the stratigraphic interval. The N-S fault system is comprised of a series of small faults oriented in different directions. Numerous faults and lineaments are also present and most of these trend NW-SE. Several small horst-grabens like structures, generated from movement against faults are very prominent from this attribute. As we move towards the top of the Woodford (Figure 9b), we observe that a NE-SW trending lineament dominates over the NW-SE trending lineaments- which might be important in the natural fracture analysis in the area. To get a better idea about the different set of lineaments present within the stratigraphic interval, their azimuth as well as change in azimuth within the strata, we studied the strike of the most-negative principal curvature, ψ_{k2}, (plotted against hue) modulated by the magnitude of the most negative principal curvature, k_2 (Figure 10). This attribute nicely delineate the change in azimuth in the large faults and series of faults within the N-S fault terrain and more importantly faults in NE-SW direction and lineaments from NW-SE direction. It also reveals the change in azimuth within a short distance. The NW-SE trending lineaments gets more oriented towards WNW as we study the horizon slice 10 ms below the top of Woodford.

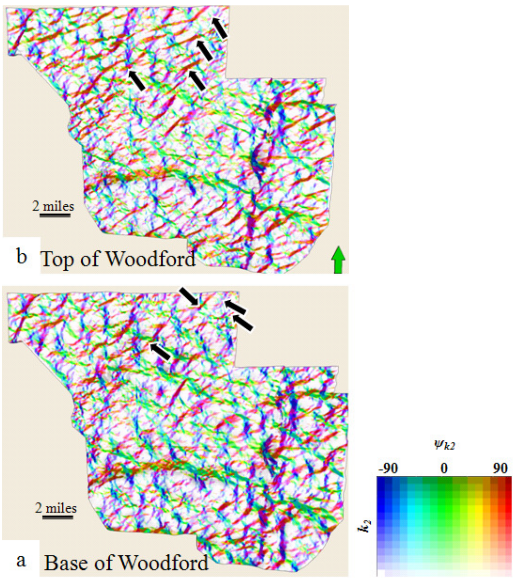

Figure 10: Horizon slice through the strike of the most-negative principal curvature, ψ_{k2}, (plotted against hue) modulated by the magnitude of the most negative principal curvature, k2. (a) 10 ms above the Hunton top and (b) near the Woodford top. Note the change in the orientation (indicated by black arrows) of the lineaments in the Woodford compared to the Hunton, indicated by black arrows.

Acknowledgements

The authors would like to thank Chesapeake Energy for providing the dataset and granting permission for this publication. Special thanks to the sponsors of the AASPI consortium for their continuous encouragement and support.